Gac is a transcriptional repressor of the Lyme disease spirochete's OspC virulence-associated surface protein

Tatiana N. Castro-Padovani [1, §], Timothy C. Saylor[1, §], Olivia T. Husted[1, § ,†], Andrew C. Krusenstjerna[1, §], and Brian Stevenson [1,2, *]

1. Department of Microbiology, Immunology, and Molecular Genetics, University of Kentucky College of Medicine, Lexington, Kentucky
2. Department of Entomology, University of Kentucky College of Agriculture, Food, and Ecology, Lexington, Kentucky

§ T.N. Castro-Padovani, T.C. Saylor, O.T. Husted, and A.C. Krusenstjerna contributed equally to this work, and are to be considered equal co-first authors

* For correspondence:
Brian Stevenson, MS421 Medical Center, Department of Microbiology, Immunology, and Molecular Genetics, University of Kentucky College of Medicine, Lexington, Kentucky, USA, 40536-0298

† Current address for O.T. Husted: Venture Laboratories, Lexington, KY

22

23 **Abstract**

24 The OspC outer-surface lipoprotein is essential for the Lyme disease spirochete's initial
25 phase of vertebrate infection. Bacteria within the midguts of unfed ticks do not produce
26 OspC, but produce high levels when ticks begin to ingest blood. Lyme disease
27 spirochetes cease production of OspC within 1-2 weeks of vertebrate infection, and
28 bacteria that fail to downregulate OspC are cleared by host antibodies. Thus, tight
29 regulation of OspC levels is critical for survival of Lyme borreliae, and therefore an
30 attractive target for development of novel treatment strategies. Previous studies
31 determined that a DNA region 5′ of the *ospC* promoter, the *ospC* operator, is required
32 for control of OspC production, but the mechanism was not determined. Hypothesizing
33 that the *ospC* operator may bind a regulatory factor, DNA affinity pulldown was
34 performed, and identified binding by the Gac protein. Gac is encoded by the C-terminal
35 half of the *gyrA* open reading frame, from an internal promoter, ribosome-binding site,
36 and initiation codon. Our analyses determined that Gac exhibits a substantially greater
37 affinity for *ospC* operator and promoter DNAs than for other tested borrelial sequences.
38 In vitro and in vivo analyses demonstrated that Gac is a transcriptional repressor of
39 *ospC*. These results constitute a substantial advance to our understanding the
40 mechanisms by which the Lyme disease spirochete controls production of OspC.

41

42 **Importance**

43 *Borrelia burgdorferi* (sensu lato) requires its surface-exposed OspC protein in order to
44 establish infection of humans and other vertebrate hosts. Lyme disease spirochetes
45 initiate production of OspC when the vector tick begins to feed on the blood of a
46 vertebrate host, and the spirochetes ceases production of OspC soon after establishment
47 of infection. Bacteria that either do not produce OspC during transmission, or fail to
48 repress OspC after infection is established, are rapidly cleared by the host. The
49 molecular mechanisms controlling OspC production are largely unstudied. Herein, we
50 identified a borrelial protein, Gac, that binds with high affinity to the *ospC* promoter
51 and 5′ adjacent DNA. A combination of biochemical analyses and investigations of
52 genetically-manipulated bacteria demonstrated that Gac is a transcriptional repressor of
53 *ospC*. This is a substantial advance toward understanding how the Lyme disease
54 spirochete controls production of the essential OspC virulence factor, and identifies a
55 novel target for preventative and curative therapies.

56

57

58 **Introduction**

59 The Lyme disease spirochete, *Borrelia burgdorferi* sensu lato (*B. burgdorferi* sl),
60 requires its OspC protein during the initial stages of vertebrate infection, and mutant
61 bacteria that cannot produce this outer surface-exposed lipoprotein are unable to
62 initiate infection of vertebrates (1-5). Production of OspC is tightly regulated. *B.*
63 *burgdorferi* sl within the midguts of unfed ticks do not express OspC (6, 7). As ticks
64 begin to feed on host blood, spirochetes initiate production of OspC, with the large
65 majority producing detectable quantities of OspC at the time of transfer from tick to
66 vertebrate (6, 8-10). The function(s) of OspC is not completely understood - it can bind a
67 tick salivary protein and vertebrate plasminogen and complement C4b - but may have
68 additional functions (11-21). Infected humans and other animals mount strong antibody
69 responses against OspC within days of infection (22-25). At the same time, *B. burgdorferi*
70 sl represses expression of OspC, and spirochetes that do not shut off OspC synthesis are
71 cleared by immunocompetent hosts (2, 3, 5, 26-30). Thus, regulation of OspC may be an
72 excellent target for novel therapeutics to prevent and/or clear *B. burgdorferi* infections.

73 OspC was the first *B. burgdorferi* sl protein to be identified as being regulated
74 during the natural tick-vertebrate infectious cycle (6). As noted above, OspC is not
75 produced in unfed ticks, but is highly expressed in feeding ticks and during the earliest
76 stages of vertebrate infection (6, 8). Regulated production can also be manipulated in
77 culture, with bacteria grown at 23˚C, pH=7.5, or culture media that yield slow
78 replication rates, producing low to no OspC, while the protein is highly expressed
79 following transfer from those conditions to 35˚C, pH=6.5, or complete culture media,

80 respectively (6, 31-33). It is not yet known how those culture conditions are interpreted
81 by *B. burgdorferi* sl to modulate OspC levels, but they provide convenient means to
82 evaluate borrelial regulatory mechanisms.

83 An alternative sigma factor, named RpoS, is also affected by the above-described
84 infection and culture conditions (33-35). RpoS controls production of numerous *B.*
85 *burgdorferi* sl proteins that are required for vertebrate infection (36, 37). Deletion of *rpoS*
86 blocks induction of OspC, which has led to a hypothesis that expression of *ospC* is solely
87 due to RpoS-RNA polymerase holoenzyme directly transcribing from the *ospC*
88 promoter (34, 38). Yet, there is evidence that transcriptional control of *ospC* is more
89 complicated than that model assumes. Previous studies found that a region of DNA 5'
90 of the *ospC* transcriptional start site, designated the *ospC* operator, is necessary for
91 induction of *ospC* transcription (39-41). The mode of function of the *ospC* operator had
92 not been defined prior to the current investigations.

93 *B. burgdorferi* sl has been divided into several clades that are often referred to as
94 genospecies, which include *B. burgdorferi* sensu stricto (*B. burgdorferi* ss) and *B. garinii*.
95 An earlier study noted that the *ospC* operator of *B. burgdorferi* ss type strain B31 includes
96 a pair of inverted repeat sequences (Fig. 1) (41). Yet, those inverted repeats are found in
97 only a subset of Lyme disease borreliae (42). However, the *ospC* operators of all
98 examined Lyme spirochetes contain two or more copies of a conserved 11bp directly-
99 repeating sequence (Fig. 1 and (42)). *B. burgdorferi* ss B31 contains two copies of the 11bp
100 repeat, which overlap the previously discussed inverted repeats (Fig. 1 and (41, 42)). In
101 contrast, the *ospC* operators of some strains of the *B. garinii* genospecies contain seven

102 adjacent copies of the 11bp repeat (Fig. 1). All *ospC* promoters also contain a copy of the
103 11bp repeat, oriented in the opposite direction (Fig. 1). The retention of the 11bp repeat
104 suggested to us that it may be a key component of *ospC* regulation, with sequence
105 conservation pointing toward it being a binding site for a regulatory protein. To address
106 that hypothesis, we performed DNA-binding studies with borrelial cytoplasmic extract,
107 identified a component protein that has high affinity for the *ospC* operator, and
108 identified a functional role for that protein as a transcriptional repressor of *ospC*.

109 **Results**

110 **Identification of Gac as an *ospC* operator-binding protein.** As a first step, an
111 infectious clone of *B. burgdorferi* ss type strain B31, B31-MI-16, was cultured to mid-
112 exponential phase at 35˚C. That condition was adopted based on our previous
113 characterization of the *B. burgdorferi erp* operons, whose expression is also responsive to
114 culture temperature, in which we found that the *erp* repressing and activating proteins
115 were all adequately expressed when cultured at 35˚C (43-45).

116 A fluorescently-tagged DNA sequence corresponding to the *ospC* operator region
117 of *B. garinii* Ip89 was incubated with the B31-MI-16 cytoplasmic extract, then subjected
118 to electrophoretic mobility shift electrophoresis (EMSA). The strain Ip89 sequence was
119 used for these analyses under the hypothesis that a protein that binds to the 11bp
120 repeated sequence would have an overall greater affinity for the 7 repeats of Ip89 as
121 opposed to the 2 repeats of B31 (Fig. 1). Addition of the cytoplasmic extract resulted in
122 retarded mobility of the labeled DNA probe, indicating that a borrelial component
123 bound to the DNA (Fig. 2A).

124 Ip89 *ospC* operator DNA was again PCR amplified, but with one of the
125 oligonucleotide primers containing a 5′ biotin moiety. That DNA was adhered to
126 streptavidin-coated magnetic beads, incubated with B31 cytoplasmic extract, washed
127 extensively, then bound proteins eluted with buffers having progressively greater
128 concentrations of NaCl. Aliquots of each eluted fraction were subjected to SDS-PAGE
129 and proteins stained with SYPRO-Ruby. A protein band with an approximate molecular
130 mass of 30-35 kDa eluted at 0.3 and 0.5 M NaCl (Fig. 2B). The bands were excised from

131 the gel, subjected to trypsin digestion and mass spectrometry, and results compared to
132 the predicted proteome of B31-MI-16. Only one potential match was obtained, to the
133 GyrA subunit of DNA gyrase, with 9 unique peptides identified. Notably, all of the
134 identified peptide fragments mapped to the C-terminal half of GyrA (Fig. 2C).

135 Bacterial DNA gyrases are comprised of two subunits, GyrA and GyrB (46).
136 GyrA proteins possess a unique C-terminal domain that bends DNA to facilitate the
137 topoisomerase activity of the gyrase (47, 48). Curiously, Lyme disease borreliae produce
138 two separate proteins from the *gyrA* locus, a full length GyrA protein and a second, 35
139 kDa protein named Gac, which is transcribed from an internal promoter and consists
140 solely of the C-terminal DNA-binding domain (48-50) (Fig. 2D, and Fig. S1). The
141 function(s) of Gac was previously unknown. We pursued the possibility that Gac
142 preferentially binds to *ospC* operator DNA and thereby affects production of OspC.

143

144 **Gac exhibits high-affinity binding to the *ospC* operator and promoter.** The Gac
145 protein was first detected by methods similar to ours, in a DNA-affinity pull-down
146 study using a *B. burgdorferi* plasmid telomere sequence (49). That study observed that
147 recombinant Gac could also bind to other DNA sequences, and so it was hypothesized
148 that binding of Gac lacked specificity (49). We note, however, that the previous report
149 did not state the concentrations of recombinant Gac or DNA probes used in their
150 EMSAs, nor were results shown. The brief description of methods in that publication do
151 not mention use of unlabeled competitor DNAs, which can also be critical to

152 determining binding specificity. We therefore conducted comparative analyses to assess
153 the relative affinity of Gac for *ospC* operator sequences and other DNAs.

154 To address that question, labeled DNA probes were constructed that consisted of
155 either the strain Ip89 or B31 *ospC* operators (Fig. 1). Additional unlabeled DNAs were
156 produced for use as EMSA competitors: each of the *ospC* operators, truncated segments
157 of the B31 *ospC* operator, and DNA sequences corresponding to the 5′ ends of the
158 borrelial *flaB* and *ospAB* operons. The Ip89 *ospC* operator probe and competitor were
159 derived by PCR from plasmid pCR2.1 clones, using plasmid-specific M13 Reverse and
160 Forward primers, so an additional unlabeled competitor was produced by PCR of
161 empty pCR2.1, to account for vector-derived DNA sequences.

162 EMSAs of the Ip89 *ospC* operator probe and recombinant Gac found that the
163 protein bound to the labeled probe (Fig 3A, lane 2). Addition of 10-times excess of
164 unlabeled Ip89 *ospC* operator partly depleted the DNA-Gac EMSA band, while 25-fold
165 excess of unlabeled Ip89 *ospC* operator completely eliminated the complex (Fig. 3A,
166 lanes 3 and 4, respectively). Addition of 25-times excess unlabeled B31 *ospC* operator
167 had little effect on the Ip89 operator-Gac complex, indicating a greater affinity of Gac
168 for the Ip89 operator than for the B31 operator (Fig 3A, lane 5). Note that the primary
169 difference between the Ip89 and B31 DNAs is the number of 11bp repeat sequences in
170 their *ospC* operators. Inclusion of 25-fold excesses of either empty pCR2.1 amplicon,
171 *flaB*, or *ospAB* unlabeled DNAs did not compete Gac away from the labeled probe (Fig
172 3A, lanes 6, 7, and 8, respectively). Thus, Gac displays substantially greater affinity for
173 the Ip89 *ospC* operator than it does for any of the other tested sequences.

174 Similar EMSAs were performed with labeled B31 *ospC* operator as probe.
175 Unlabeled B31 *ospC* operator DNA effectively competed Gac away from the labeled
176 probe (Fig 3B, lanes 3-4). Inclusion of 10-fold excesses of the empty pCR2.1 amplicon,
177 *flaB*, or *ospAB* unlabeled DNAs exhibited lower levels of competition for Gac binding
178 (Fig 3B, lanes 5, 6, and 7, respectively). However, 25-fold excess of all of those unlabeled
179 DNA competed Gac away from the labeled B31 *ospC* labeled probe (data not shown).
180 These results indicate that Gac binds to the B31 *ospC* operator with a greater affinity
181 than to the *flaB, ospAB,* or pCR2.1 competitor sequences, but has a lower affinity for the
182 B31 *ospC* operator than for the Ip89 *ospC* operator.
183 Using labeled *ospC* operator from strain B31 as the EMSA probe, truncated
184 segments of that DNA region were used as competitors to narrow down the sequences
185 that bound Gac (Fig 4). As above, 10- and 25-fold excesses of unlabeled B31 *ospC*
186 operator DNA competed Gac away from the labeled probe. Since the labeled probe
187 included vector sequences at each end, competitor A was designed to contain only *ospC*
188 operator sequences; it also effectively competed for Gac-binding at 10-fold excess. Of
189 the other competitors, D yielded the greatest level of competition, while B, C, F, and G
190 competed to lesser extents. These results indicate that Gac also has an elevated affinity
191 for the *ospC* promoter region. We note that the space between the *ospC* -10 and -35
192 sequences includes an 11bp sequence that resembles the operator repeat (Figure 1).
193
194 **Altered *ospC* expression in *gac* mutant *B. burgdorferi*.** To assess the effects of
195 Gac in live *B. burgdorferi*, *gac* mutant strain CKO-1, strain CKO-1 (pBLS820) (CKO-1

196 complemented with wild-type *gac*), and strain NGR (an isogenic wild-type *gac* clone)
197 were cultured to mid-exponential phase at 23 ˚C, then diluted into fresh media and
198 incubated to mid-exponential phase at 35 ˚C (6, 31). Immunoblot analyses of lysates of
199 the 23 and 35˚C cultures using OspC-specific antibodies found that all three strains
200 exhibited differential expression of OspC protein, with substantially greater amounts of
201 OspC being synthesized at 35 ˚C (Fig. 5). However, Gac-deficient strain CKO-1
202 produced 14- and 1.4-times more OspC than did NGR at 23 and 34˚C, respectively. The
203 greatest net impact was observed with the 23˚C cultures, consistent with Gac being a
204 repressor of OspC synthesis. Complementation of CKO-1 with a wild-type *gac* gene on
205 pBLS820 reduced OspC levels by 32% and 20% at 23 and 34˚C, respectively. The
206 complemented strain did not fully return to wild-type OspC levels, suggesting that the
207 minimal *gac* promoter in pBLS820 does not contain all of the cis elements necessary for
208 normal control of *gac* expression.

209 *B. burgdorferi* strains NGR and CKO-1 were next transformed with plasmids that
210 carry transcriptional fusions between B31 *ospC* operator/promoter sequences and *gfp*.
211 Plasmid pBLS761 carries the same operator/promoter sequence that was used as the
212 EMSA probe in the above-described studies, while pBLS764 lacks the 11 bp direct
213 repeats (equivalent to the sequences of competitors A and G in Fig. 4, respectively).
214 Each transformant was cultured at 35˚C to mid-exponential phase, then bacterial GFP
215 content was assessed by flow cytometry (Fig. 6). CKO-1(pBLS761) produced
216 substantially greater levels of GFP than did NGR(pBLS761), consistent with the
217 observed levels of OspC protein and transcript described above.

218 NGR(pBLS764), which lacks the *ospC* operator, did not produce GFP (Fig. 6). In
219 contrast, CKO-1(pBLS764) produced GFP at levels comparable to CKO-1(pBLS761). We
220 conclude that absence of Gac relieves transcriptional repression of the *ospC* promoter,
221 while the *ospC* operator is also required for efficient transcription from the *ospC*
222 promoter if Gac is present. Those results suggest that one or more additional factors
223 interact with *ospC* operator DNA to inhibit Gac binding to the *ospC* promoter. Studies
224 are ongoing to examine that hypothesis.
225
226 ***B. burgdorferi* regulates transcription of *gac*.** Since *ospC* is induced in *B.*
227 *burgdorferi* cultured at 35˚C, we assessed *ospC* and *gyrA/gac* transcript levels over time in
228 cultures of wild-type *B. burgdorferi* (Fig. 7). Levels of *ospC* transcript increased as the
229 cultures grew through exponential into stationary phase. The two *gyrA/gac* primer sets
230 yielded different Q-RT-PCR results for each pair. Since the 5′ primers detected mRNA
231 that only encoded *gyrA*, whereas the 3′ primers detected both *gyrA* and *gac* mRNAs, the
232 relative concentration of *gac* mRNA was approximated by subtracting the results of 5′
233 Q-RT-PCR from results from the 3′ primer set. The concentration of Gac-encoding
234 transcript was greatest during lag and early exponential phases, then declined as the
235 cultures matured and entered stationary phase. Those changes were opposite of *ospC*,
236 and are consistent with the above-described results that indicate Gac is a repressor of
237 *ospC*.
238

239 **Gac exhibits affinity for the telomere of *B. burgdorferi* B31 plasmid lp17.**
240 *Borrelia* species contain both circular and linear DNAs, and there is considerable interest
241 in the mechanisms by which the spirochetes maintain linear replicons (51-53). The Gac
242 protein was initially identified through an affinity pull-down method similar to ours,
243 using a bait sequence derived from a telomere of strain B31's linear plasmid lp17 (49).
244 Having found that Gac binds to *ospC* 5′ DNAs with high degrees of affinity, we
245 revisited the previous study. A labeled DNA probe with the same telomere-derived
246 sequence was produced, then assessed by EMSA for ability to bind Gac in the presence
247 of excess levels of various unlabeled DNAs. Recombinant Gac produced an EMSA shift
248 with the labeled telomere probe, which was effectively competed away with 10-fold and
249 25-fold excesses of unlabeled telomere sequence (Fig. 8, lanes 2-4). Ten-fold excesses of
250 unlabeled Ip89 or B31 *ospC* operator DNAs also competed Gac away from the labeled
251 telomere DNA (Fig. 8, lanes 6 and 7, respectively). Unlabeled empty pCR2.1 amplicon
252 partly competed for Gac binding, while neither the *flaB* nor the *ospAB* DNAs detectably
253 competed (Fig. 8, lanes 5, 8, and 9, respectively). We conclude that Gac actually does
254 exhibit specific affinity for the lp17 telomere region, although its relative affinity is
255 lower than for the Ip89 and B31 *ospC* operators, yet higher than for the examined *ospAB*
256 or *flaB* DNA sequences.
257
258

259 **Discussion**

260 These studies found that Gac binds with high affinity to *ospC* promoter and
261 operator DNA, and inhibits transcription. Deletion of the *ospC* operator did not alleviate
262 Gac-dependent repression of transcription from the *ospC* promoter, suggesting that Gac
263 binding to the promoter itself is sufficient to repress transcription. The *ospC* operator is
264 evidently necessary for relief of Gac-dependent transcriptional repression, mirroring
265 results from previous studies that also found that the operator is essential for regulation
266 of *ospC* transcription (39-41). Thus, it appears that a "factor(s) X" interacts with the *ospC*
267 operator and somehow prevents repression by Gac (Fig. 9). We are currently pursuing
268 biochemical and genetic routes to identify the hypothesized factor X.

269 Gac was initially identified because it bound to a telomere of linear plasmid lp17
270 (49), although it was not studied further due to perceived lack of binding specificity.
271 The present analyses indicate that Gac actually has a marked preference for the lp17
272 telomere. This raises questions about the function(s) of Gac in *B. burgdorferi*. Our studies
273 found that Gac has elevated affinity for three sites in the *B. burgdorferi* genome – the
274 *ospC* operator, the *ospC* promoter, and the telomere of lp17 – yet can also possesses
275 lesser affinity for other DNA sequences. Gac wraps DNA around itself, forming 180-
276 220˚ bends (48). Taken together, these data suggest that Gac may be a nucleoid-
277 associated protein (NAP, or "histone-like protein"). Supporting that model, Gac
278 complements some features of the *E. coli* NAP HU when expressed in that species (49,
279 50). It is not uncommon for NAPs to also influence transcription (54-56). Indeed, the

280 antirepressor of *B. burgdorferi erp* operon transcription, EbfC, meets the criteria of being
281 an NAP (57).

282 At this time, it is not known whether production of a separate Gac protein from
283 the 3′ end of the *gyrA* ORF is unique to *B. burgdorferi*. The possibility that *gyrA* can
284 encode two distinct proteins has never been addressed for the vast majority of other
285 bacterial species. It would be worth examining other *gyrA* genes for presence of
286 potential ribosome binding sites and start codons near the beginning of the C-terminal
287 domain.

288 In conclusion, our investigations found that *B. burgdorferi* Gac has elevated
289 affinity for *ospC* operator and promoter DNAs. Gac repressed *ospC* transcription in vitro
290 and in live spirochetes. Levels of *ospC* and *gac* transcripts changed in opposite directions
291 during cultivation, consistent with *ospC* repression by Gac. Analyses of mutants
292 indicate that the *ospC* operator is required to alleviate Gac repression of the *ospC*
293 promoter, implying that one or more additional factors interact with the *ospC* operator
294 to prevent repression by Gac. That protein also bound with elevated affinity to an lp17
295 telomere, suggesting that Gac might play a role in linear DNA maintenance.
296

297 **Materials and Methods**

298 **Bacteria, plasmids, and culture conditions.** *B. burgdorferi* sensu stricto strain B31
299 is the type strain, and was isolated from an *Ixodes scapularis* tick that was collected on
300 Shelter Island, New York (58, 59). Infectious clone B31-MI-16 was used to prepare
301 cytoplasmic extracts for identification of *ospC* operator-binding proteins (60). *B. garinii*
302 strain Ip89 was isolated from an *I. persulcatus* tick that was collected in central Eurasia
303 (61, 62).

304 *Borrelia* spp. strains were cultured in BSK-II broth at either 23 or 35˚C (63).
305 Temperature shift cultivation was performed by diluting a 23˚C culture 1:100 into fresh
306 medium, then incubating at 35˚C (31). Culture densities were determined with a Petroff-
307 Hausser counting chamber and dark field microscopy.

308 Analyses of the effects of Gac on OspC expression used a Δ*gac* clone of strain
309 B31, CKO-1, and an isogenic control strain, NGR (50). The overlap of the *gac* ORF with
310 the essential *gyrA* ORF precludes outright deletion of the *gac* locus. For that reason,
311 Knight et al. (50) produced *gac* defective strain CKO-1 by an allelic exchange mutation
312 that changed the two potential *gac* start codons from ATG to CTT and ATT (leucine and
313 isoleucine, respectively) and the ribosome binding site from AGGAGG to AGAAGA.
314 The mutant does not produce a Gac protein, although it does produce normal levels of
315 GyrA (50). The *gac* mutations were selected by simultaneous introduction of point
316 mutations into the adjacent *gyrB* gene, which confer resistance to coumermycin (50, 64).
317 The CKO-1 *gac* mutant exhibits growth patterns that are physiologically

318 indistinguishable from the wild-type parent or from NGR, an isogenic coumermycin-
319 resistant *gyrB* strain (50).

320 Plasmid pBLS820 was custom produced by GenScript (Piscataway, NJ) by
321 cloning the *B. burgdorferi gac* open reading frame, ribosome-binding site, and promoter
322 into vector pBSV2-G (65) (Fig. S1). *B. burgdorferi* CKO-1 was transformed by
323 electroporation, and transformants were selected by culture in 150 μg/ml gentamicin.

324 Plasmid pBLS761 contains the B31 *ospC* promoter and operator in a
325 transcriptional fusion with *gfp*. Plasmid pBLS764 is identical to pBLS761 except that it
326 lacks the *ospC* operator. Both are based on pBLS740, which was produced for this work
327 by cloning the *gfp* gene of pBLS590 between the BamHI and HindIII sites of vector
328 pKFSS1 (66, 67). The *ospC*-derived DNAs used to make pBLS761 and pBLS764 were
329 inserted between the KpnI and BamHI sites of pBLS740, custom synthesized by
330 GenScript. Two of our previously-described plasmids were used as GFP expression
331 controls: KS10, which carries a promoterless *gfp* on pBLS590, and KS20, which carries
332 the constitutively-expressed minimal *erpAB* promoter driving *gfp* on pBLS599 (66).
333 Plasmids pBLS590 and pBLS599 confer resistance to kanamycin. *B. burgdorferi*
334 containing pBLS590 or pBLS599 were cultured in media that contained 200 μg/ml
335 kanamycin, while spirochetes that contain pBLS761 or pBLS764 were cultured in media
336 with 50 μg/ml streptomycin (66-69).

337

338 **Cytoplasmic extracts.** *B. burgdorferi* ss B31-MI-16 was cultured at 35˚C to mid-
339 exponential phase (approximately $5x10^7$ bacteria/ml). Bacteria were harvested by

340 centrifugation, washed with phosphate buffered saline (PBS), and resuspended in a
341 minimal volume of 50mM Tris (pH=7.6), 10mM EDTA, 10% (w/vol) sucrose. The
342 suspension was frozen in a dry ice/ ethanol bath, then allowed to thaw in an ice-water
343 bath. NaCl, dithiothreitol, and lysozyme were added to final concentrations of 140 mM,
344 1 mM, and 0.4 mg/ml, respectively, and incubated on ice for 5 min. The cell mixture
345 was subjected to four additional freeze-thaw cycles. Cellular debris was pelleted by
346 centrifugation, and the supernatant was aliquoted and stored at -80˚C (70).
347
348 **Electrophoretic mobility shift assays (EMSAs).** Labeled and unlabeled nucleic
349 acids are described in Supplementary Table 1. Fluorescently tagged IRDye800 labeled
350 probes were utilized for EMSAs. For each EMSA binding reaction, a labeled probe was
351 incubated for 15 min at room temperature with protein and unlabeled competitor DNA
352 as necessary, in EMSA buffer (50mM Tris-HCl, 25mMKCl, 10% glycerol (vol/vol),
353 0.01% Tween 20, 100nM dithiothreitol, and 1mM phenylmethanesulfonyl fluoride
354 (PMSF). Protein-nucleic acid mixtures were then loaded into either 6% or 10% Novex
355 TBE gels (Thermo Fisher). Gels were pre-run for at least 30 min at 100V in 0.5x TBE
356 buffer before sample loading. Following the addition of the samples, electrophoresis
357 was conducted for up to 1.5 h at 100V.
358 Initially, a fragment of *B. garinii* Ip89 DNA, from 5' of the *ospC* operator through
359 the *ospC* promoter, was amplified from genomic DNA by PCR with oligonucleotide
360 primers 1021 and 1022 (Supplementary Table 1). The resulting amplicon was cloned
361 into pCR2.1 (Invitrogen) to create pBLS756. Fluorescently-tagged IP89 *ospC* operator

362 was produced by PCR of pBLS756 using IRDye800-tagged M13-Reverse and unlabeled
363 M13-Forward primers (Supplementary Table 1). The probe was incubated with cleared
364 borrelial cytoplasmic extract in EMSA buffer for 15 min at room temperature with 10ng
365 poly-dI-dC, then subjected to electrophoresis.

366 Other EMSAs used purified recombinant Gac protein, labeled *ospC*
367 operator/promoter probes, and unlabeled DNA competitors.

368 In addition, a sub-telomeric sequence of strain B31 lp17 was amplified from total
369 genomic DNA by PCR with oligonucleotides TL16h and TL16g as previously described
370 (49). The resulting PCR product was cloned into pCR2.1 (Invitrogen) and maintained in
371 *E. coli* TOP-10. The amplicon was completely sequenced on both strands to ensure
372 fidelity. Fluorescently tagged telomere probe was produced by PCR using IRDye800
373 tagged M13-Reverse and unlabeled M13-Forward primers.

374

375 **DNA affinity pull-down.** Proteins that bind *ospC* operator DNA were purified
376 from B31-MI-16 cytoplasmic extracts as previously described (71). Briefly, bacteria of a
377 mid-exponential phase (approximately $5x10^7$ bacteria/ml) culture were harvested,
378 washed, and frozen at -80˚C. Bacterial pellets were then thawed on ice, and subjected to
379 three additional rounds of freezing at -80˚C / thawing on ice. Bacterial lysates were
380 resuspended in a minimal volume of BS/THES buffer (44.3% THES buffer, 20% BS
381 buffer, 35.7% water). THES Buffer consists of 50mM Tri HCl (pH 7.5), 10mM EDTA,
382 20% sucrose (w/vol), 140mM NaCl, 0.7% (vol/vol) Protease Inhibitor Cocktail II

383 (Sigma), and 0.1% (vol/vol) Phosphatase Inhibitor Cocktail II (Sigma). BS buffer
384 consists of 50mM HEPES (pH=7.5), 25mM $CaCl_2$, 250mM KCl, and 60% (vol/vol)
385 glycerol. Suspended bacteria were lysed by sonication, on ice. Cellular debris was
386 pelleted by centrifugation, and the supernatant was divided into aliquots.
387
388 **Recombinant Gac protein.** The B31 *gac* ORF was cloned into pET101, then
389 sequenced to confirm fidelity. C-terminally His-tagged Gac was expressed in *E. coli*
390 Rosetta II upon induction with 1 mM of isopropyl-β-d-thiogalactopyranoside (IPTG) for
391 1 hour at 37°C. Bacteria were collected by centrifugation, and the pellet was frozen at -
392 80°C. The bacterial pellet was then thawed on ice, resuspended in phosphate buffered
393 saline (PBS) containing 10 mM imidazole, and bacteria lysed by sonication. The sonicate
394 was subjected to centrifugation, then recombinant protein purified from the soluble
395 fraction using a HisPur Ni-NTA (Thermo Scientific) column. Purified protein was
396 dialyzed against EMSA buffer. Protein concentration was determined by Bradford assay
397 and purity assessed by SDS-PAGE with Coomassie brilliant blue staining.
398
399 **Immunoblot analyses.** Cultures of strains NGR, CKO-1, and CKO-1(pBLS820)
400 were harvested at mid-exponential phase by centrifugation, then split into aliquots for
401 immunoblot assays and RNA extraction. Pellets for immunoblot assays were frozen at -
402 80°C, subsequently thawed at room temperature, then resuspended in 10% SDS, boiled
403 for 5-minutes, and vigorously vortexed. The resulting lysates were stored at 4°C. Prior
404 to electrophoresis, samples were preheated to 42° before adding to 2x sodium dodecyl

405 sulfate (SDS)-page loading dye (63mM Tris pH7.5, 18.75% w/v glycerol, 10% w/v 2-
406 mercaptoethanol, 4% SDS, and .5% w/v bromophenol blue). Separation by SDS-
407 polyacrylamide gel electrophoresis was followed by electrotransfer to nitrocellulose
408 membranes and blocking with 5% nonfat dried milk in Tris-buffered saline-Tween-20
409 (20 mM Tris [pH 7.5], 150 mM NaCl, 0.05% [vol/vol] Tween-20). The membranes were
410 then incubated with murine monoclonal antibodies directed against FlaB or OspC (72,
411 73). After incubation with primary antibodies, membranes were incubated with goat
412 anti-mouse IgG conjugated to IRDye800 (LI-Cor). Immunoblots were imaged and
413 analyzed with ChemiDoc MP and Image-Lab software, respectively (Bio-Rad, CA).
414
415 **Quantitative reverse transcription PCR (Q-RT-PCR).** *B. burgdorferi* was
416 cultured at 35 ºC, and 2 ml aliquots of bacteria were taken 1-, 3-, 5-, 7-, 9-, and 11-days
417 post-inoculation. Bacteria were pelleted, then washed two times with PBS and frozen at
418 -80 ºC. Frozen pellets were later resuspended in 60 ºC TRIzol (Thermo Fisher), and RNA
419 was extracted using Qiagen Mini RNA kits. Residual genomic DNA was depleted using
420 on-column Turbo DNase (Thermo Fisher). The quality (RIN > 7) and quantity of the
421 RNA were determined using an Agilent 2100 Bioanalyzer and Agilent 6000 Nano chips.
422 Purified RNA stocks were stored at -80 ºC.
423 Complementary DNA (cDNA) for qPCR was produced using the iScript gDNA
424 Clear cDNA synthesis kits (Bio-Rad). The cDNA stocks were diluted 1:100 into
425 nuclease-free water for use as template. Quantitative PCR was carried out using iTaq

426 Universal SYBR Green Supermix (Bio-Rad) and a Bio-Rad CFX96 Touch Real-time PCR
427 thermocycler. For all reactions, cycles involved melting at 95 ºC for 10s, annealing at 55
428 ºC for 10 s, and extension at 72 ºC for 30s. Each run was performed with technical
429 triplicates of each reaction as well as no-template control reactions that lacked template.
430 Melting curves were performed with each run to validate production of specific
431 amplicons. Every reaction was tested with a reverse transcriptase-negative template to
432 validate the absence of contaminating gDNA. Cq values were normalized to *ftsK*, a gene
433 whose expression is stable across different growth phases (74), using the ΔCq method,
434 and fold-difference was determined by the function $2^{-\Delta Cq}$.
435

Acknowledgements

This work was funded by NIH grant 3R01AI144126-03S1. We thank Nerina Jusufovic and Jessamyn Moore for constructive comments on this project and manuscript; Scott Samuels for providing *B. burgdorferi* strains NGR and CKO-1, and for helpful comments on these studies; Haining Zhu and Jing Chen for assistance with mass spectrometric analyses; Jennifer Strange, Greg Bowman, and Cuiping Zhang for flow cytometry analyses. Figure 9 was produced using BioRender.com.

446 **References**

447 1. Grimm D, Tilly K, Byram R, Stewart PE, Krum JG, Bueschel DM, Schwan TG,
448 Policastro PF, Elias AF, Rosa PA. 2004. Outer-surface protein C of the Lyme
449 disease spirochete: a protein induced in ticks for infection of mammals. Proc Natl
450 Acad Sci USA 101:3142-3147.

451 2. Stewart PE, Wang X, Bueschel DM, Clifton DR, Grimm D, Tilly K, Carroll JA,
452 Weis JJ, Rosa PA. 2006. Delineating the requirement for the *Borrelia burgdorferi*
453 virulence factor OspC in the mammalian host. Infect Immun 74:3547-3553.

454 3. Tilly K, Krum JG, Bestor A, Jewett MW, Grimm D, Bueschel D, Byram R,
455 Dorward D, Vanraden MJ, Stewart P, Rosa P. 2006. *Borrelia burgdorferi* OspC
456 protein is required exclusively in a crucial early stage of mammalian infection.
457 Infect Immun 74:3554-3564.

458 4. Tilly K, Bestor A, Jewett MW, Rosa P. 2007. Rapid clearance of Lyme disease
459 spirochetes lacking OspC from skin. Infect Immun 75:1517-1519.

460 5. Tilly K, Bestor A, Rosa PA. 2013. Lipoprotein succession in *Borrelia burgdorferi*:
461 similar but distinct roles for OspC and VlsE at different stages of mammalian
462 infection. Mol Microbiol 89:216-227.

463 6. Schwan TG, Piesman J, Golde WT, Dolan MC, Rosa PA. 1995. Induction of an
464 outer surface protein on *Borrelia burgdorferi* during tick feeding. Proc Natl Acad
465 Sci USA 92:2909-2913.

466 7. Fingerle V, Hauser U, Liegl G, Petko B, Preac-Mursic V, Wilske B. 1995.
467 Expression of outer surface proteins A and C of *Borrelia burgdorferi* in *Ixodes*
468 *ricinus*. J Clin Microbiol 33:1867-1869.

469 8. Schwan TG, Piesman J. 2000. Temporal changes in outer surface proteins A and
470 C of the Lyme disease-associated spirochete, *Borrelia burgdorferi*, during the chain
471 of infection in ticks and mice. J Clin Microbiol 38:382-388.

472 9. Pal U, Yang X, Chen M, Bockenstedt LK, Anderson JF, Flavell RA, Norgard MV,
473 Fikrig E. 2004. OspC facilitates *Borrelia burgdorferi* invasion of *Ixodes scapularis*
474 salivary glands. J Clin Invest 113:220-230.

475 10. Skare JT, Shaw DK, Trzeciakowski JP, Hyde JA. 2016. In vivo imaging
476 demonstrates that *Borrelia burgdorferi ospC* is uniquely expressed temporally and
477 spatially throughout experimental infection. PLoS ONE 11:e0162501.

478 11. Lagal V, Portnoï D, Faure G, Postic D, Baranton G. 2006. *Borrelia burgdorferi* sensu
479 stricto invasiveness is correlated with OspC-plasminogen affinity. Microbes
480 Infect 8:645-652.

481 12. Önder Ö, Humphrey PT, McOmber B, Korobova F, Francella N, Greenbaum DC,
482 Brisson D. 2012. OspC is potent plasminogen receptor on surface of *Borrelia*
483 *burgdorferi*. J Biol Chem 287:16860-16868.

484 13. Ramamoorthi N, Narasimhan S, Pal U, Bao F, Yang XF, Fish D, Anguita J,
485 Norgard MV, Kantor FS, Anderson JF, Koski RA, Fikrig E. 2005. The Lyme
486 disease agent exploits a tick protein to infect the mammalian host. Nature
487 436:573-577.

488 14. Xu Q, McShan K, Liang FT. 2008. Essential protective role attributed to the
489 surface lipoproteins of *Borrelia burgdorferi* against innate defences. Mol Microbiol
490 69:15-29.

491 15. Earnhart CG, Leblanc DV, Alix KE, Desrosiers DC, Radolf JD, Marconi RT. 2010.
492 Identification of residues within ligand-binding domain 1 (LBD1) of the *Borrelia*
493 *burgdorferi* OspC protein required for function in the mammalian environment.
494 Mol Microbiol 76:393-408.

495 16. Antonara S, Ristow P, McCarthy J, Coburn J. 2010. Effect of *Borrelia burgdorferi*
496 OspC at the site of inoculation in mouse skin. Infect Immun 78:4723-4733.

497 17. Caine JA, Coburn J. 2015. A short-term *Borrelia burgdorferi* infection model
498 identifies tissue tropisms and bloodstream survival conferred by adhesion
499 proteins. Infect Immun 83:3184-3194.

500 18. Carrasco SE, Troxell B, Yang Y, Brandt SL, Li H, Sandusky GE, Condon KW,
501 Serezani CH, Yang XF. 2015. Outer surface protein OspC is an antiphagocytic
502 factor that protects *Borrelia burgdorferi* from phagocytosis by macrophages. Infect
503 Immun 83:4848-4860.

504 19. Caine JA, Lin YP, Kessler JR, Sato H, Leong JM, Coburn J. 2017. *Borrelia*
505 *burgdorferi* outer surface protein C (OspC) binds complement component C4b
506 and confers bloodstream survival. Cell Microbiol 19:10.1111/cmi.12786.

507 20. Bierwagen P, Szpotkowski K, Jaskolski M, Urbanowicz A. 2019. *Borrelia* outer
508 surface protein C is capable of human fibrinogen binding. FEBS J 286:2415-2428.

509 21. Lin YP, Tan X, Caine JA, Castellanos M, Chaconas G, Coburn J, Leong JM. 2020.
510 Strain-specific joint invasion and colonization by Lyme disease spirochetes is
511 promoted by outer surface protein C. PLoS Pathog 16:e1008516.

512 22. Fuchs R, Jauris S, Lottspeich F, Preac-Mursic V, Wilske B, Soutschek E. 1992.
513 Molecular analysis and expression of a *Borrelia burgdorferi* gene encoding a 22kDa
514 protein (pC) in *Escherichia coli*. Mol Microbiol 6:503-509.

515 23. Fung BP, McHugh GL, Leong JM, Steere AC. 1994. Humoral immune response to
516 outer surface protein C of *Borrelia burgdorferi* in Lyme disease: role of the
517 immunoglobulin M response in the serodiagnosis of early infection. Infect
518 Immun 62:3213-3221.

519 24. Padula SJ, Dias F, Sampieri A, Craven RB, Ryan RW. 1994. Use of recombinant
520 OspC from *Borrelia burgdorferi* for serodiagnosis of early Lyme disease. J Clin
521 Microbiol 32:1733-1738.

522 25. Gilmore RD, Kappel KJ, Dolan MC, Burkot TR, Johnson BJB. 1996. Outer surface
523 protein C (OspC), but not P39, is a protective immunogen against a tick-
524 transmitted *Borrelia burgdorferi* challenge: evidence for a conformational
525 protective epitope in OspC. Infect Immun 64:2234-2239.

526 26. Liang FT, Jacobs MB, Bowers LC, Philipp MT. 2002. An immune evasion
527 mechanism for spirochetal persistence in Lyme borreliosis. J Exp Med 195:415-
528 422.

529 27. Crother TR, Champion CI, Whitelegge JP, Aguilera R, Wu XY, Blanco DR, Miller
530 JN, Lovett MA. 2004. Temporal analysis of the antigenic composition of *Borrelia*
531 *burgdorferi* during infection in rabbit skin. Infect Immun 72:5063-5072.

532 28. Liang FT, Yan J, Mbow ML, Sviat SL, Gilmore RD, Mamula M, Fikrig E. 2004.
533 *Borrelia burgdorferi* changes its surface antigenic expression in response to host
534 immune reponses. Infect Immun 72:5759-5767.

535 29. Xu Q, Seemanapalli SV, McShan K, Liang FT. 2006. Constitutive expression of
536 outer surface protein C diminishes the ability of *Borrelia burgdorferi* to evade
537 specific humoral immunity. Infect Immun 74:5177-5184.

538 30. Tilly K, Bestor A, Dulebohn DP, Rosa PA. 2009. OspC-independent infection and
539 dissemination by host-adapted *Borrelia burgdorferi*. Infect Immun 77:2672-2682.

540 31. Stevenson B, Schwan TG, Rosa PA. 1995. Temperature-related differential
541 expression of antigens in the Lyme disease spirochete, *Borrelia burgdorferi*. Infect
542 Immun 63:4535-4539.

543 32. Carroll JA, Garon CF, Schwan TG. 1999. Effects of environmental pH on
544 membrane proteins in *Borrelia burgdorferi*. Infect Immun 67:3181-3187.

545 33. Jutras BL, Chenail AM, Stevenson B. 2013. Changes in bacterial growth rate
546 govern expression of the *Borrelia burgdorferi* OspC and Erp infection-associated
547 surface proteins. J Bacteriol 195:757-764.

548 34. Hübner A, Yang X, Nolen DM, Popova TG, Cabello PC, Norgard MV. 2001.
549 Expression of *Borrelia burgdorferi* OspC and DbpA is controlled by a RpoN-RpoS
550 regulatory pathway. Proc Natl Acad Sci USA 98:12724-12729.

551 35. Caimano MJ, Groshong AM, Belperron A, Mao J, Hawley KL, Luthra A, Graham
552 DE, Earnhart CG, Marconi RT, Bockenstedt LK, Blevins JS, Radolf JD. 2019. The
553 RpoS gatekeeper in *Borrelia burgdorferi*: an invariant regulatory scheme that
554 promotes spirochete persistence in reservoir hosts and niche diversity. Front
555 Microbiol 10:1923.

556 36. Burtnick MN, Downey JS, Brett PJ, Boylan JA, Frye JG, Hoover TR, Gherardini
557 FC. 2007. Insights into the complex regulation of *rpoS* in *Borrelia burgdorferi*. Mol
558 Microbiol 65:277-293.

559 37. Caimano MJ, Iyer R, Eggers CH, Gonzalez C, Morton EA, Gilbert MA, Schwartz
560 I, Radolf JD. 2007. Analysis of the RpoS regulon in *Borrelia burgdorferi* in response
561 to mammalian host signals provides insight into RpoS function during the
562 enzootic cycle. Mol Microbiol 65:1193-1217.

563 38. Yang XF, Lybecker MC, Pal U, Alani SM, Blevins J, Revel AT, Samuels DS,
564 Norgard MV. 2005. Analysis of the *ospC* regulatory element controlled by the
565 RpoN-RpoS regulatory pathway in *Borrelia burgdorferi*. J Bacteriol 187:4822-4829.

566 39. Xu Q, McShan K, Liang FT. 2007. Identification of an *ospC* operator critical for
567 immune evasion of *Borrelia burgdorferi*. Mol Microbiol 64:220-231.

568 40. Xu Q, McShan K, Liang FT. 2008. Verification and dissection of the *ospC* operator
569 by using *flaB* promoter as a reporter in *Borrelia burgdorferi*. Microb Pathog 45:70-
570 78.

571 41. Drecktrah D, Hall LS, Hoon-Hanks LL, Samuels DS. 2013. An inverted repeat in
572 the ospC operator is required for induction in *Borrelia burgdorferi*. PLoS One
573 8:e68799.

574 42. Tilly K, Casjens S, Stevenson B, Bono JL, Samuels DS, Hogan D, Rosa P. 1997. The
575 *Borrelia burgdorferi* circular plasmid cp26: conservation of plasmid structure and
576 targeted inactivation of the *ospC* gene. Mol Microbiol 25:361-373.

577 43. Babb K, Bykowski T, Riley SP, Miller MC, DeMoll E, Stevenson B. 2006. *Borrelia*
578 *burgdorferi* EbfC, a novel, chromosomally-encoded protein, binds specific DNA
579 sequences adjacent to *erp* loci on the spirochete's resident cp32 prophages. J
580 Bacteriol 188:4331-4339.

581 44. Burns LH, Adams CA, Riley SP, Jutras BL, Bowman A, Chenail AM, Cooley AE,
582 Haselhorst LA, Moore AM, Babb K, Fried MG, Stevenson B. 2010. BpaB, a novel
583 protein encoded by the Lyme disease spirochete's cp32 prophages, binds to *erp*
584 Operator 2 DNA. Nucleic Acids Res 38:5443-5455.

585 45. Jutras BL, Chenail AM, Carroll DW, Miller MC, Zhu H, Bowman A, Stevenson B.
586 2013. Bpur, the Lyme disease spirochete's PUR-domain protein: identification as
587 a transcriptional modulator and characterization of nucleic acid interactions. J
588 Biol Chem 288:26220-26234.

589 46. Sugino A, Higgins NO, Cozzarelli NR. 1908. DNA gyrase subunit stoichiometry
590 and the covalent attachment of subunit A to DNA during DNA cleavage. Nucleic
591 Acids Res 8:3865-3874.

592 47. Reece RJ, Maxwell A. 1991. The C-terminal domain of the *Escherichia coli* DNA
593 gyrase A subunit is a DNA-binding protein. Nucleic Acids Res 19:1399-1405.

594 48. Corbett KD, Shultzaberger RK, Berger JM. 2004. The C-terminal domain of DNA
595 gyrase A adopts a DNA-bending beta-pinwheel fold. Proc Natl Acad Sci USA
596 101:7293-7298.

597 49. Knight SW, Samuels DS. 1999. Natural synthesis of a DNA-binding protein from
598 the C-terminal domain of DNA gyrase A in *Borrelia burgdorferi*. EMBO J 18:4875-
599 4881.

600 50. Knight SW, Kimmel BJ, Eggers CH, Samuels DS. 2000. Disruption of the *Borrelia*
601 *burgdorferi gac* gene, encoding the naturally synthesized GyrA C-terminal
602 domain. J Bacteriol 182:2048-2051.

603 51. Barbour AG, Garon CF. 1987. Linear plasmids of the bacterium *Borrelia*
604 *burgdorferi* have covalently closed ends. Science 237:409-411.

605 52. Fraser CM, Casjens S, Huang WM, Sutton GG, Clayton R, Lathigra R, White O,
606 Ketchum KA, Dodson R, Hickey EK, Gwinn M, Dougherty B, Tomb J-F,
607 Fleischmann RD, Richardson D, Peterson J, Kerlavage AR, Quackenbush J,
608 Salzberg S, Hanson M, van Vugt R, Palmer N, Adams MD, Gocayne J,
609 Weidmann J, Utterback T, Watthey L, McDonald L, Artiach P, Bowman C,
610 Garland S, Fujii C, Cotton MD, Horst K, Roberts K, Hatch B, Smith HO, Venter

611 JC. 1997. Genomic sequence of a Lyme disease spirochaete, *Borrelia burgdorferi*.
612 Nature 390:580-586.

613 53. Casjens S, Palmer N, van Vugt R, Huang WM, Stevenson B, Rosa P, Lathigra R,
614 Sutton G, Peterson J, Dodson RJ, Haft D, Hickey E, Gwinn M, White O, Fraser C.
615 2000. A bacterial genome in flux: the twelve linear and nine circular
616 extrachromosomal DNAs of an infectious isolate of the Lyme disease spirochete
617 *Borrelia burgdorferi*. Mol Microbiol 35:490-516.

618 54. Dorman CJ, Schumacher MA, Bush MJ, Brennan RG, Buttner MJ. 2020. When is a
619 transcription factor a NAP? Curr Opin Microbiol 55:26-33.

620 55. Amemiya HM, Schroeder J, Freddolino PL. 2021. Nucleoid-associated proteins
621 shape chromatin structure and transcriptional regulation across the bacterial
622 kingdom. Transcription 12:182-218.

623 56. Muskhelishvili G, Sobetzko P, Mehandziska S, Travers A. 2021. Composition of
624 transcription machinery and its crosstalk with nucleoid-associated proteins and
625 global transcription factors. Biomolecules 11:924.

626 57. Jutras BL, Bowman A, Brissette CA, Adams CA, Verma A, Chenail AM,
627 Stevenson B. 2012. EbfC (YbaB) is a new type of bacterial nucleoid-associated
628 protein, and a global regulator of gene expression in the Lyme disease
629 spirochete. J Bacteriol 194:3395-3406.

630 58. Burgdorfer W, Barbour AG, Hayes SF, Benach JL, Grunwaldt E, Davis JP. 1982.
631 Lyme disease - a tick-borne spirochetosis? Science 216:1317-1319.

632 59. Johnson RC, Schmid GP, Hyde FW, Steigerwalt AG, Brenner DJ. 1984. *Borrelia*
633 *burgdorferi* sp. nov.: etiologic agent of Lyme disease. Int J Syst Bacteriol 34:496-
634 497.

635 60. Miller JC, von Lackum K, Babb K, McAlister JD, Stevenson B. 2003. Temporal
636 analysis of *Borrelia burgdorferi* Erp protein expression throughout the mammal-
637 tick infectious cycle. Infect Immun 71:6943-6952.

638 61. Xu Y, Johnson RC. 1995. Analysis and comparison of plasmid profiles of *Borrelia*
639 *burgdorferi* sensu lato strains. J Clin Microbiol 33:2679-2685.

640 62. Kraiczy P, Seling A, Brissette CA, Rossmann E, Hunfeld K-P, Bykowski T, Burns
641 LH, Troese MJ, Cooley AE, Miller JC, Brade V, Wallich R, Casjens S, Stevenson B.
642 2008. *Borrelia burgdorferi* complement regulator-acquiring surface protein 2
643 (CspZ) as a serological marker of human Lyme disease. Clin Vaccine Immunol
644 15:484-491.

645 63. Zückert WR. 2007. Laboratory maintenance of *Borrelia burgdorferi*. Curr Protoc
646 Microbiol 12C:1-10.

647 64. Samuels DS, Mach KE, Garon CF. 1994. Genetic transformation of the Lyme
648 disease agent *Borrelia burgdorferi* with coumarin-resistant *gyrB*. J Bacteriol
649 176:6045-6049.

650 65. Elias AF, Bono JL, Kupko JJ, Stewart PE, Krum JG, Rosa PA. 2003. New antibiotic
651 resistance cassettes suitable for genetic studies in *Borrelia burgdorferi*. J Mol
652 Microbiol Biotechnol 6:29-40.

653 66. Babb K, McAlister JD, Miller JC, Stevenson B. 2004. Molecular characterization of
654 *Borrelia burgdorferi erp* promoter/operator elements. J Bacteriol 186:2745-2756.

655 67. Frank KL, Bundle SF, Kresge ME, Eggers CE, Samuels DS. 2003. *aadA* confers
656 streptomycin resistance in *Borrelia burgdorferi*. J Bacteriol 185:6723-6727.

657 68. Bono JL, Elias AF, Kupko JJ, Stevenson B, Tilly K, Rosa P. 2000. Efficient targeted
658 mutagenesis in *Borrelia burgdorferi*. J Bacteriol 182:2445-2452.

659 69. Stewart PE, Thalken R, Bono JL, Rosa P. 2001. Isolation of a circular plasmid
660 region sufficient for autonomous replication and transformation of infectious
661 *Borrelia burgdorferi*. Mol Microbiol 39:714-721.

662 70. Babb K, El-Hage N, Miller JC, Carroll JA, Stevenson B. 2001. Distinct regulatory
663 pathways control the synthesis of *Borrelia burgdorferi* infection-associated OspC
664 and Erp surface proteins. Infect Immun 69:4146-4153.

665 71. Jutras BL, Verma A, Stevenson B. 2012. Identification of novel DNA-binding
666 proteins using DNA-affinity chromatography/pull down. Curr Protocols
667 Microbiol 1F:1-13.

668 72. Barbour AG, Hayes SF, Heiland RA, Schrumpf ME, Tessier SL. 1986. A *Borrelia*-
669 specific monoclonal antibody binds to a flagellar epitope. Infect Immun 52:549-
670 554.

671 73. Mbow ML, Gilmore RD, Stevenson B, Golde WT, Piesman J, Johnson BJB. 2002.
672 *Borrelia burgdorferi*-specific monoclonal antibodies derived from mice primed
673 with Lyme disease spirochete-infected *Ixodes scapularis* ticks. Hybrid
674 Hybridomics 21:179-182.

675 74. Arnold WK, Savage CR, Brissette CA, Seshu J, Livny J, Stevenson B. 2016. RNA-
676 Seq of *Borrelia burgdorferi* in Multiple Phases of Growth Reveals Insights into the
677 Dynamics of Gene Expression, Transcriptome Architecture, and Noncoding
678 RNAs. PLoS One 11:e0164165.

679

680

681

682

683 **Figure Legends**

684

685 **Figure 1.** Alignment of the DNA sequences 5′ of the *ospC* ORFs of *B. burgdorferi* ss B31
686 and *B. garinii* Ip89, which includes the *ospC* operator (39-41). Both strains contain
687 multiple copies of an 11bp repeated sequence (blue arrows), with Ip89 carrying seven
688 directly repeated copies. Additionally, both strains contain an inverted copy of this
689 sequence between their -35 and -10 promoter elements. A previous study noted an
690 inverted repeat sequence in the operator of strain B31 (red arrows), which is not found
691 in strain Ip89 or many other Lyme disease borreliae (41, 42).

692

693 **Figure 2. (A)** Electrophoretic mobility shift assay (EMSA) of labeled Ip89 *ospC* operator,
694 without (-) and with (+) cytoplasmic extract from strain B31. The asterisk indicates
695 shifted probe that was present only when borrelial extract was included, indicating
696 presence of a DNA-binding component. Unbound DNA is indicated by "free". Some
697 labeled DNA probe remained in the wells of the gel. **(B)** Cytoplasmic extract from strain
698 B31 was incubated with Ip89 *ospC* operator DNA affixed to beads, eluted with
699 increasing concentrations of NaCl, and eluates were separated by SDS-polyacrylamide
700 gel electrophoresis. Lanes are labeled with the concentration of NaCl used for that
701 elution. The arrow indicated a protein band of 30-35 kDa that eluted in the 0.3 and 0.5
702 mM NaCl washes. **(C)** Amino acid sequence of GyrA and Gac (the two potential
703 initiation methionines of Gac are indicated by boldface and underlining). Mass
704 spectrometry identified nine unique peptides that all mapped to the Gac ORF. Peptides

705 identified with high confidence are shaded green, and those with lower confidence in
706 red. **(D)** Predicted structures of *B. burgdorferi* Gac and GyrA proteins, as determined by
707 AlphaFold (https://alphafold.ebi.ac.uk). Both are consistent with the solved structures
708 of *B. burgdorferi* Gac (48) and the N-terminal domain of *E. coli* GyrA
709 (https://www.rcsb.org/structure/4CKK).
710
711 **Figure 3.** EMSAs of purified recombinant Gac with labeled *ospC* operator DNAs and
712 unlabeled competitors. Shifted DNAs are indicated with asterisks. Unoccupied DNAs
713 are labeled "free". **(A)** Labeled Ip89 operator (100 nM) without (lane 1) and with 25 nM
714 Gac (lanes 2-8). Lane 2: no added competitor. Lane 3: plus 10x excess unlabeled Ip89
715 *ospC* operator. Lane 4: plus 25x excess unlabeled Ip89 *ospC* operator. Lane 5: plus 25x
716 excess unlabeled B31 *ospC* operator. Lane 6: plus 25x unlabeled pCR2.1 amplicon. Lane
717 7: plus 25x excess unlabeled *flaB* DNA. Lane 8: plus 25x unlabeled *ospAB* DNA. **(B)**
718 Labeled B31 operator (100 nM) without (lane 1) and with 25 nM Gac (lanes 2-7). Lane 2:
719 no added competitor. Lane 3: plus 10x excess unlabeled B31 *ospC* operator. Lane 4: plus
720 25x excess unlabeled B31 *ospC* operator. Lane 5: plus 10x unlabeled pCR2.1 amplicon.
721 Lane 6: plus 10x excess unlabeled *flaB* DNA. Lane 7: plus 10x unlabeled *ospAB* DNA.
722
723 **Figure 4.** Mapping Gac binding sites in B31 *ospC* 5′ DNA by EMSA with purified
724 recombinant Gac and unlabeled competitor DNA fragments. Sequences of the probe
725 and competitors are shown above the EMSA, with the 11bp repeats indicated by blue
726 arrows. Shifted DNAs are indicated with asterisks. Unoccupied DNAs are labeled

727 "free". Labeled B31 operator (100 nM) without (lane 1) and with 25 nM Gac (lanes 2-11).
728 Lane 2: no added competitor. Lane 3: plus 10x excess unlabeled B31 *ospC* operator
729 probe. Lane 4: plus 25x excess unlabeled B31 *ospC* operator probe. Lanes 5-11: plus 10x
730 unlabeled competitors A through G, respectively.
731
732 **Figure 5.** Western blot analyses of strains NGR, CKO-1, and CKO-1(pBLS820) that were
733 cultured to mid-exponential phase at 23 or 35˚C, probed with monospecific antibodies
734 against OspC and FlaB. In the illustrated experiment, strain CKO-1 produced 14-times
735 and 1.4-times more OspC than did NGR at 23 and 34˚C, respectively. Complementation
736 of CKO-1 with a wild-type *gac* gene on pBLS820 led to 32% and 20% reduction in OspC
737 at 23 and 34˚C, respectively.
738
739 **Figure 6.** Flow cytometric analyses of green fluorescent protein (GFP) levels. Each panel
740 represent approximately 100,000 bacteria. Isogenic NGR and *gac* mutant CKO-1
741 contained transcriptional fusions of the *ospC* promoter, with an without the operator
742 (pBLS761 and pBLS764, respectively), fused to *gfp*. Negative control strain KS10 carries
743 promoterless *gfp* on pBLS590, and positive control strain KS20 carries the constitutive
744 *erpAB* promoter fused to *gfp* on pBLS599 (66). *B. burgdorferi* were cultured to mid-
745 exponential phase at 35˚C.
746
747 **Figure 7.** Growth curves and quantitative-RT-PCR analyses of selected transcripts of *B.*
748 *burgdorferi* B31, cultured at 35˚C. Bacterial cell densities are indicated by black squares

749 and lines. Relative transcript levels are indicated by red circles and lines. **(A)** Schematic
750 of the locations of amplicons used to determine relative expression of the 5' and 3'
751 portions of *gyrA*. The 5' primer pair amplify only transcripts arising from the promoter
752 5' of *gyrB*, while the 3' primer pair amplify transcripts arising from both the promoter 5'
753 of *gyrB* and within the *gyrA* ORF. **(B)** Results from the 5' segment of *gyrA*. **(C)** Results from
754 the 3' segment of *gyrA*. **(D)** Results from the *gyrA* 3' segment minus the *gyrA* 5'. **(E)**
755 Analyses of *ospC* transcript levels.
756
757 **Figure 8.** EMSAs of purified recombinant Gac with labeled *ospC* lp17 telomere DNA
758 and competitors. Shifted DNAs are indicated with asterisks. Unoccupied DNA is
759 labeled "free". All lanes contain 100mM labeled lp17 telomere probe, without (lane 1)
760 or with 25 nM Gac (lanes 2-9). Lane 2: no added competitor. Lane 3: plus 10x excess
761 unlabeled lp17 telomere. Lane 4: plus 25x excess unlabeled lp17 telomere. Lane 5: plus
762 10x unlabeled pCR2.1 amplicon. Lane 6: plus 10x excess unlabeled Ip89 *ospC* operator.
763 Lane 7: plus 10x excess unlabeled B31 *ospC* operator. Lane 8: plus 10x excess unlabeled
764 *flaB* DNA. Lane 9: plus 10x unlabeled *ospAB* DNA.
765
766 **Figure 9.** Graphic summary of these results. Gac binds at or near the 11bp repeated
767 sequences in the *ospC* promoter and operator, and inhibits transcription from the *ospC*
768 promoter. Deletion of the *ospC* operator resulted in ablation of transcription from the
769 *ospC* promoter, as has also been noted previously (39-41). Those data indicate that
770 another factor, "X", interacts with the *ospC* operator and is required to activate

771 transcription. In the absence of Gac, the *ospC* promoter is transcribed at high levels,
772 indicating that "X" competes against Gac repression. X may be one or more protein or
773 other factor. The 11bp repeat sequences are indicated by blue arrows beneath the DNA.
774 The *ospC* promoter -10 and -35 sequences are indicated by black bars above the DNA.
775 The
776

777 **Supplemental Material**

778

779 **Figure S1.** Sequence of the *gac* 5′ and open reading frame, which was cloned between
780 the KpnI and BamHI sites of vector pKFSS1 to produce pBLS820. The -10 and -13 sites
781 of the transcriptional promoter and the ribosome binding site (RBS) are indicated in
782 purple. The *gac* open reading frame probably begins at the 5′-most ATG (methionine)
783 codon, although a second, downstream ATG codon could also be used. Both of those
784 initiation codons, and the RBS, were mutated in *B. burgdorferi* strain CKO-1, which
785 prevented production of Gac protein (50). The TAA termination codon of *gac* is shown
786 in red.

787

788 **Table S1.** Oligonucleotide primers used in this study.

789

```
B31   GCATATTTGGCTTTGCTTATGTCGATTTTAAAATCAAATTAAGA
Ip89  GCATATTTGGCTTTGCTTCTGTCAATCTTATAATCAATTAAGAT

B31   CAATATTTTTCAAATTCTT CAATATTTATT
Ip89  AGTTCGTTTGTAATATTTT CAATAATTATT CAATAATTTTT CAATAATTTTT CAATAATTATT CAATAATTATT GAAAAATTATT CAAATTTATTT

                                                  -35                  -10
B31   CAAGATATTGAAGAATTTGAAAAAATTATTTTTTCAAATAAAAAATTGAAAAA CAAAATTGTTG GACTAATAATTCATAAATAAAAAGGAGG
Ip89  ---------------ATTGAAAAATTATTTTTTTTATATAAAGAATTGAAAAG AAAAATTGTTG GACTAATAATTTATATAAAAAGGAGG
```

Figure 1

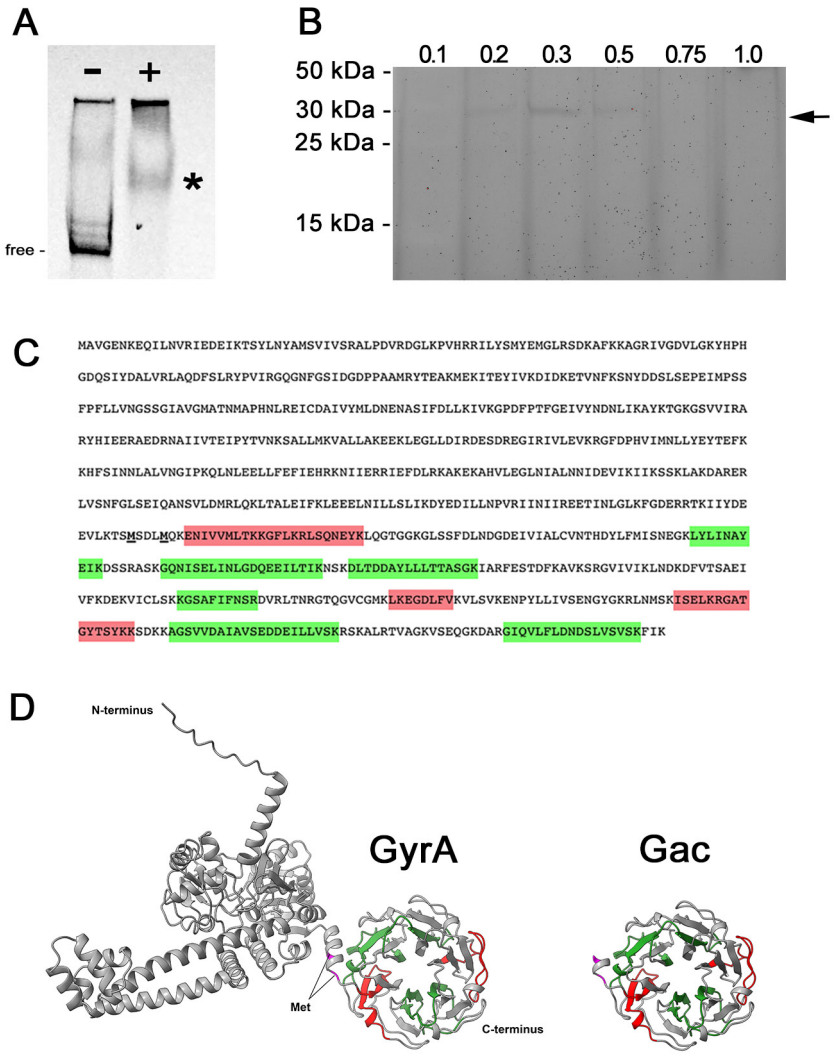
A
-
+
*
free -
B
0.1
0.2
0.3
0.5
0.75
1.0
50 kDa -
30 kDa -
25 kDa -
15 kDa -
C
MAVGENKEQILNVRIEDEIKTSYLNYAMSVIVSRALPDVRDGLKPVHRRILYSMYEMGLRSDKAFKKAGRIVGDVLGKYHPH
GDQSIYDALVRLAQDFSLRYPVIRGQGNFGSIDGDPPAAMRYTEAKMEKITEYIVKDIDKETVNFKSNYDDSLSEPEIMPSS
FPFLLVNGSSGIAVGMATNMAPHNLREICDAIVYMLDNENASIFDLLKIVKGPDFPTFGEIVYNDNLIKAYKTGKGSVVIRA
RYHIEERAEDRNAIIVTEIPYTVNKSALLMKVALLAKEEKLEGLLDIRDESDREGIRIVLEVKRGFDPHVIMNLLYEYTEFK
KHFSINNLALVNGIPKQLNLEELLFEFIEHRKNIIERRIEFDLRKAKEKAHVLEGLNIALNNIDEVIKIIKSSKLAKDARER
LVSNFGLSEIQANSVLDMRLQKLTALEIFKLEEELNILLSLIKDYEDILLNPVRIINIIREETINLGLKFGDERRTKIIYDE
EVLKTSMSDLMQKENIVVMLTKKGFLKRLSQNEYKLQGTGGKGLSSFDLNDGDEIVIALCVNTHDYLFMISNEGKLYLINAY
EIKDSSRASKGQNISELINLGDQEEILTIKNSKDLTDDAYLLLTTASGKIARFESTDFKAVKSRGVIVIKLNDKDFVTSAEI
VFKDEKVICLSKKGSAFIFNSRDVRLTNRGTQGVCGMKLKEGDLFVKVLSVKENPYLLIVSENGYGKRLNMSKISELKRGAT
GYTSYKKSDKKAGSVVDAIAVSEDDEILLVSKRSKALRTVAGKVSEQGKDARGIQVLFLDNDSLVSVSKFIK
D
N-terminus
GyrA
Gac
Met
C-terminus

Figure 2

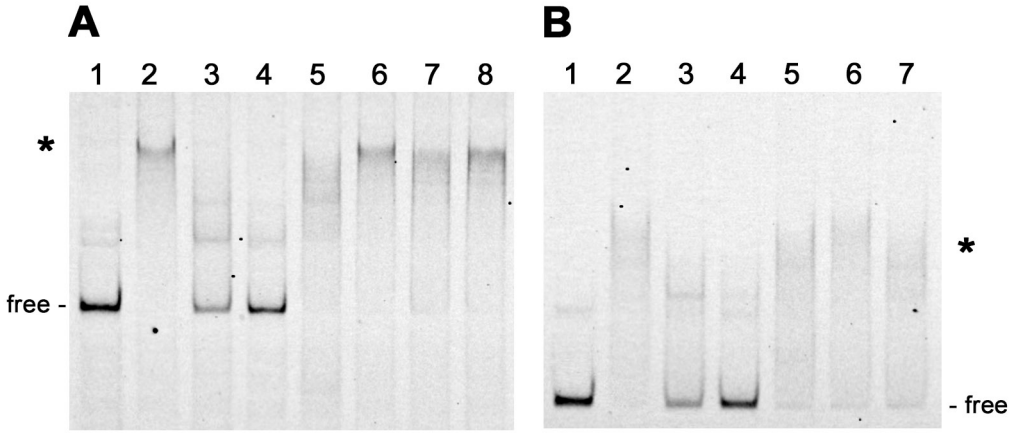

Figure 3

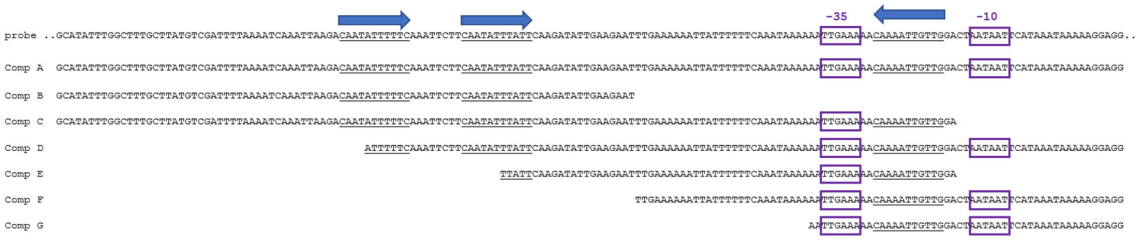
-35
-10
probe ..GCATATTTGGCTTTGCTTATGTCGATTTTAAAATCAAATTAAGACAATATTTTTCAAATTCTTCAATATTTATTCAAGATATTGAAGAATTTGAAAAAATTATTTTTTCAAATAAAAAATTGAAAAACAAAATTGTTGGACTAATAATTCATAAATAAAAAGGAGG..
Comp A GCATATTTGGCTTTGCTTATGTCGATTTTAAAATCAAATTAAGACAATATTTTTCAAATTCTTCAATATTTATTCAAGATATTGAAGAATTTGAAAAAATTATTTTTTCAAATAAAAAATTGAAAAACAAAATTGTTGGACTAATAATTCATAAATAAAAAGGAGG
Comp B GCATATTTGGCTTTGCTTATGTCGATTTTAAAATCAAATTAAGACAATATTTTTCAAATTCTTCAATATTTATTCAAGATATTGAAGAAT
Comp C GCATATTTGGCTTTGCTTATGTCGATTTTAAAATCAAATTAAGACAATATTTTTCAAATTCTTCAATATTTATTCAAGATATTGAAGAATTTGAAAAAATTATTTTTTCAAATAAAAAATTGAAAAACAAAATTGTTGGA
Comp D ATTTTTCAAATTCTTCAATATTTATTCAAGATATTGAAGAATTTGAAAAAATTATTTTTTCAAATAAAAAATTGAAAAACAAAATTGTTGGACTAATAATTCATAAATAAAAAGGAGG
Comp E TTATTCAAGATATTGAAGAATTTGAAAAAATTATTTTTTCAAATAAAAAATTGAAAAACAAAATTGTTGGA
Comp F TTGAAAAAATTATTTTTTCAAATAAAAAATTGAAAAACAAAATTGTTGGACTAATAATTCATAAATAAAAAGGAGG
Comp G AATTGAAAAACAAAATTGTTGGACTAATAATTCATAAATAAAAAGGAGG

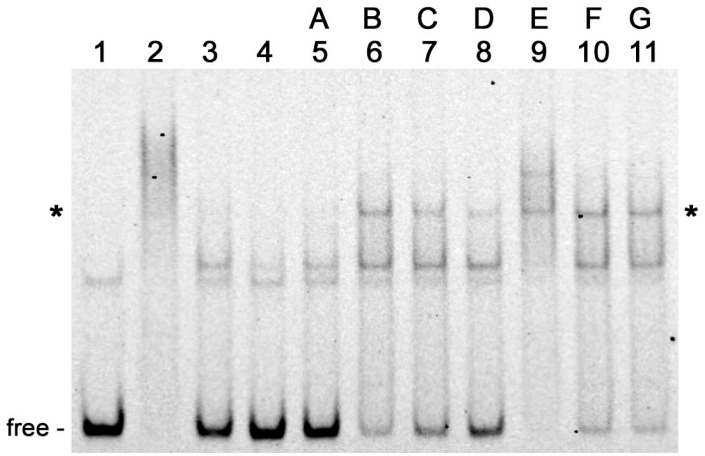
1 2 3 4 A 5 B 6 C 7 D 8 E 9 F 10 G 11
*
*
free -

Figure 4

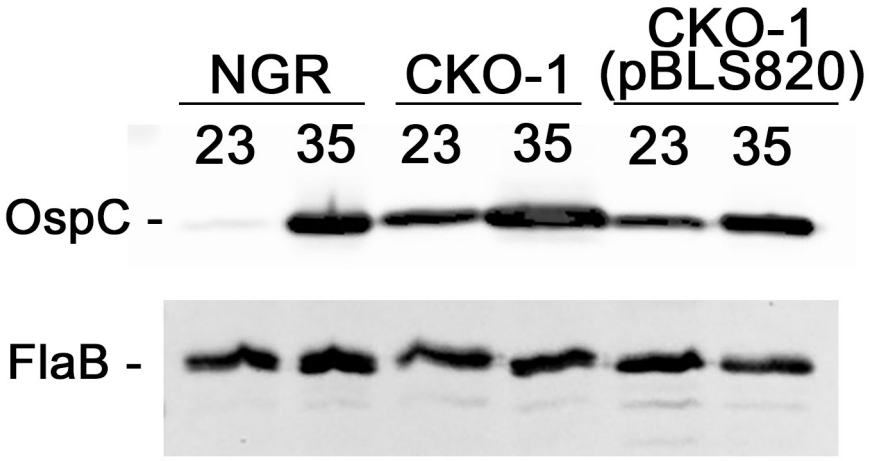

Figure 5

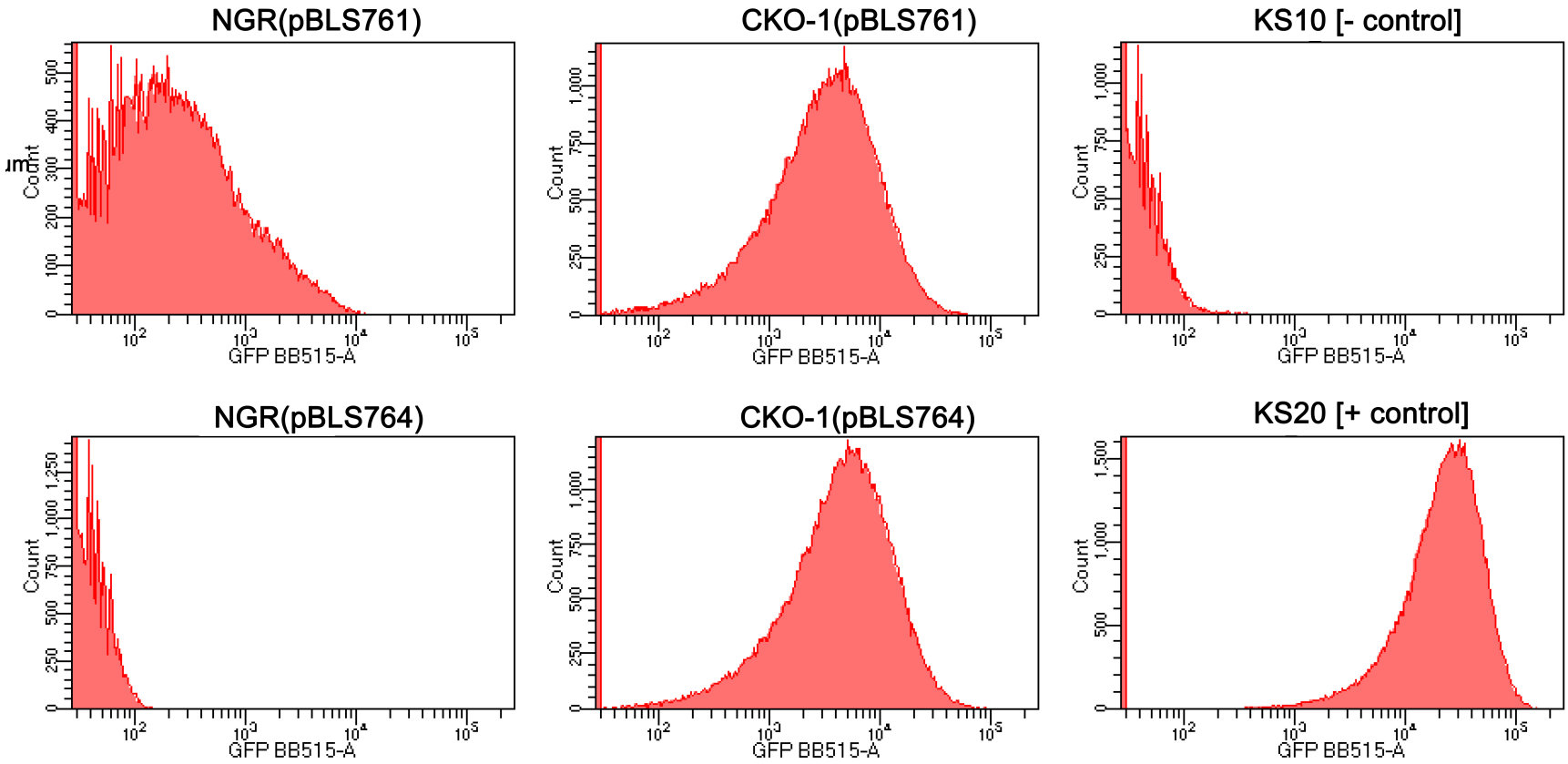
NGR(pBLS761)
CKO-1(pBLS761)
KS10 [- control]
NGR(pBLS764)
CKO-1(pBLS764)
KS20 [+ control]
Count
GFP BB515-A

Figure 6

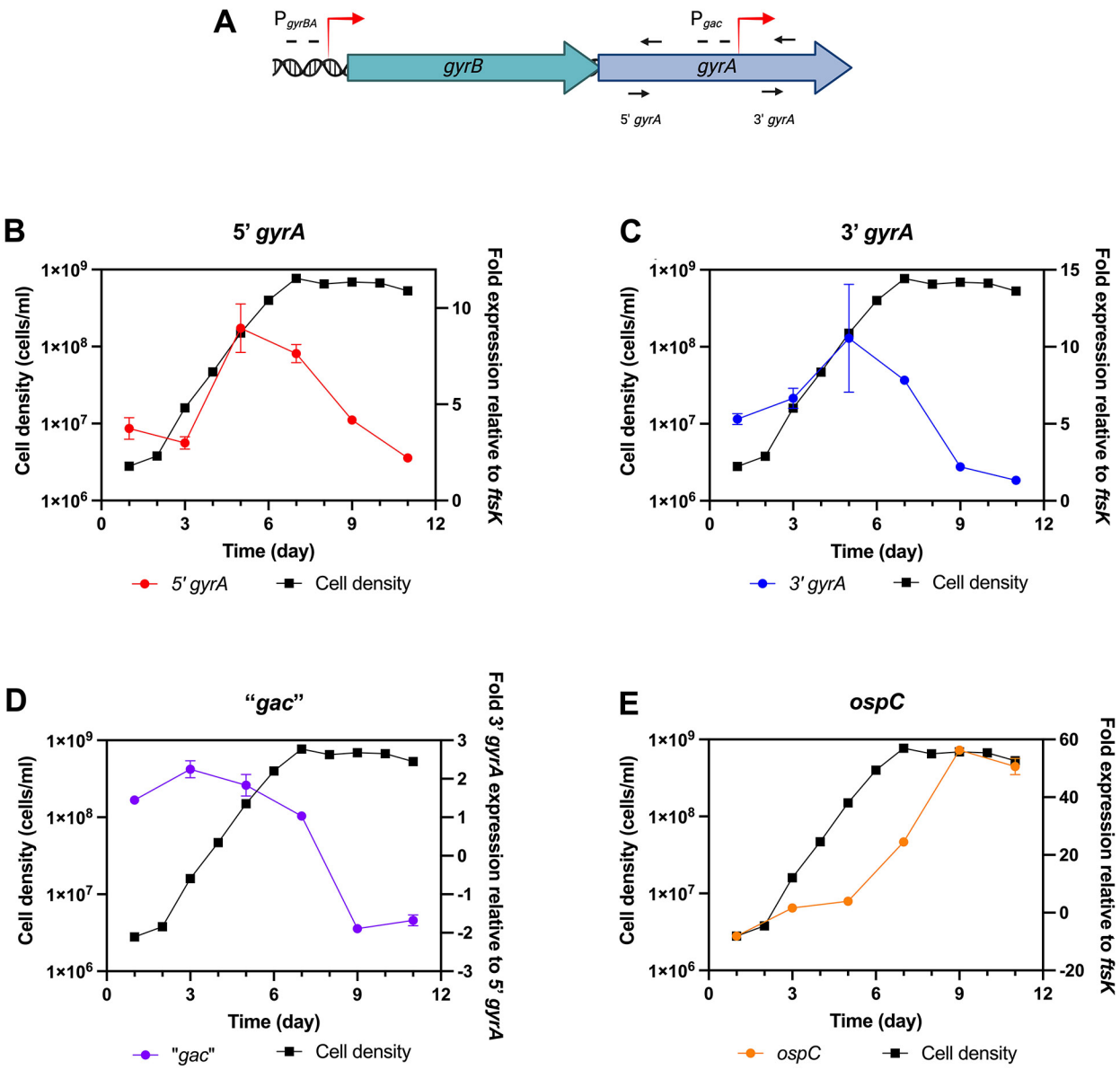
A
P_{gyrBA}
P_{gac}
gyrB
gyrA
5' gyrA
3' gyrA
B
5' gyrA
Cell density (cells/ml)
Fold expression relative to ftsK
Time (day)
5' gyrA
Cell density
C
3' gyrA
Cell density (cells/ml)
Fold expression relative to ftsK
Time (day)
3' gyrA
Cell density
D
"gac"
Cell density (cells/ml)
Fold 3' gyrA expression relative to 5' gyrA
Time (day)
"gac"
Cell density
E
ospC
Cell density (cells/ml)
Fold expression relative to ftsK
Time (day)
ospC
Cell density

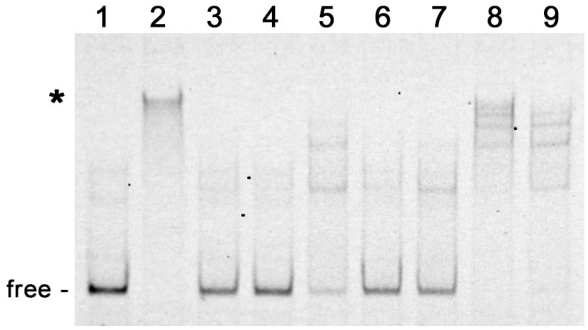

Figure 8

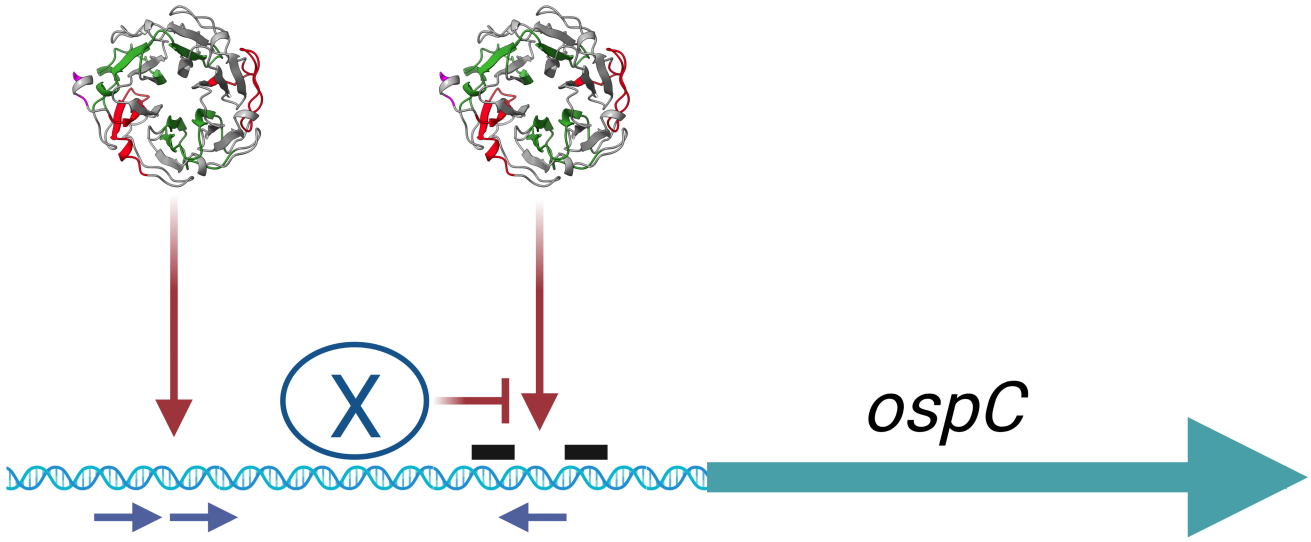

Figure 9